Journal of Thermal Analysis and Calorimetry (2018) 134:2041–2048
https://doi.org/10.1007/s10973-018-7308-6

Thermal decomposition mechanism of piroxicam

Cheng-Jie Wu[1] · Jin-Zong You[1] · Xue-Jie Wang[1]

Received: 2 February 2018 / Accepted: 14 April 2018 / Published online: 24 April 2018

Abstract
Piroxicam (PRX) is a nonsteroidal anti-inflammatory drug. The thermal decomposition process of PRX was investigated with thermogravimetry and differential scanning calorimetry. The gaseous products generated by thermal decomposition were characterized with thermogravimetric analysis coupled with Fourier transform infrared spectroscopy. The residues of the thermal decomposition at various temperatures were identified with infrared spectroscopy. The molecular bond orders were calculated using an ab initio method from the GAMESS program of quantum chemistry. The mechanism of thermal decomposition for PRX was discussed. The results indicated that the thermal decomposition of PRX is a two-stage process with the initial temperature of 198 °C either in nitrogen or air atmospheres. The thermal decompositions of the first stage in two atmospheres are the same process. The main part of the molecule, including sulfamide, amide, benzene ring and pyridine ring, decompose simultaneously and to form gasifiable small molecules and carbonaceous residue in the first stage. The second stage in nitrogen is a slow thermal pyrolysis process of carbonaceous residue. The forepart of the second stage in air is a slow thermal pyrolysis process as like as in nitrogen, and the later period of the second stage is an oxidation (combustion) reaction process of carbonaceous residue. PRX is stable under ambient temperature and air atmosphere, and it can be preserved for long-term storage under ambient temperature and in air atmosphere.

Keywords Piroxicam (PRX) · Thermal decomposition mechanism · TGA–FTIR · Quantum chemistry

Introduction

Osteoarthritis (OA) is the most common type of arthritis of the knees and hips; about 3.8% of people around the world suffered from OA in 2010 [1]. If only elderly people (over 60 years of age) are considered, about 10 and 18% of males and females, respectively, are affected by OA [2]. OA is a degenerative joint disease that can induce cartilage loss, subchondral sclerosis, inflammation of the synovium, and damage to the supporting structures of the joint [3]. As a result, pain and stiffness of the joint is the main symptom of OA. For the management of OA, lifestyle changes, including exercise and mass loss, and oral administration of nonsteroidal anti-inflammatory drugs (NSAIDs) which reduce pain and inflammation are mainly used [4]. Piroxicam (PRX), whose chemical name is 4-hydroxy-2-methyl-*N*-(2-pyridinyl)-2*H*-1,2-benzothiazine-3-carboxamide-1,1-dioxide, belongs to oxicam NSAIDs with a long plasma half-life, may be a good choice for the treatment of inflammation and pain that results from rheumatoid arthritis and OA, especially for elderly OA patients [5]. PRX also shows chemopreventive and chemosuppressive effects in different cancer cell lines and animal models, even though it is not clear exactly how they exert their anticancer effects [6–9].

Thermoanalytical techniques have been widely applied in the pharmaceutical research, such as the thermal stability and degradation of drug substances [10], the physicochemical characteristics of natural raw material [11], crystal forms and polymorphic stability [12, 13], compatibility of drug and excipients [14], correlation of drug components [15] and so on.

The degradation process and degradation products of PRX in aqueous solutions [16–18] and the thermal stability and thermal decomposition kinetics of PRX [19] have been studied, but the thermal degradation mechanism of PRX has not been reported. Now, the thermal decomposition processes of PRX in nitrogen and air atmospheres have

✉ Xue-Jie Wang
xjwang@zisu.edu.cn

[1] School of Science and Technology, Zhejiang International Studies University, Hangzhou 310012, China

been examined using thermogravimetry (TG) and differential scanning calorimetry (DSC). The volatile species that evolved during thermal decomposition was identified using coupled with infrared spectroscopy (TG–FTIR). Residues of thermal decomposition at different stages were analyzed using IR spectrometry. Molecular bond orders of GTB were calculated using an ab initio quantum chemistry program. The thermal decomposition mechanism of PRX was discussed.

Experimental

Reagents

PRX (HPLC purity $\geqq$ 98%) was purchased from Aladdin Chemistry Co. Ltd. (Shanghai, China), was used as received without any additional purification and was kept as suggested by the supplier (2–8 °C).

Experimental methods

The TG, DTG and DSC curves for PRX thermal decomposition were obtained using an SDT-Q600 simultaneous thermal analyzer (TA Instruments Inc., USA) under a continuous flow of nitrogen or air (100 mL min^{-1}) and heating rate of 10 °C min^{-1} from ambient to 800 °C. 5 ± 0.3 mg samples were weighted in open alpha-alumina crucible.

The residues from thermal decomposition were prepared in an SDT-Q600 simultaneous thermal analyzer using an alpha-alumina ceramic crucible containing PRX sample under nitrogen at a flow rate of 100 mL min^{-1} and heating rate of 10 °C min^{-1} from room temperature to the selected temperature. Endpoints included the beginning of mass loss, peak of DTG curve, and end of the first mass loss.

The TG–FTIR analysis was conducted using an SDT-Q600 Thermal Analyzer coupled with a Nicolet iS10 FTIR spectrophotometer (Thermo Fisher Scientific Inc., USA) equipped with a stainless steel transfer line and gas cell. Approximately 10 mg of sample was heated from room temperature to 800 °C at 20 °C min^{-1}. These experiments were carried out in dry nitrogen, and the flow rate of gases into the TG–FTIR cell was 100 mL min^{-1}. Both the gas cell for IR detection and the connection line transferring evolved gases from TG to FTIR were both kept at 220 °C to prevent gas condensation. The IR spectra of the evolved gases were collected at 4 cm^{-1} resolution with co-adding of 32 scans per spectrum from 4000 to 500 cm^{-1}. The three-dimensional diagrams of infrared absorption and the Gram–Schmidt (GS) curves were obtained using the software attached to the spectrometer.

The IR spectra of PRX and solid residues of thermal decomposition were obtained using a Nicolet iS10 FTIR spectrophotometer. The spectra were collected by accumulating 32 scans at a resolution of 4 cm^{-1} from 4000 to 400 cm^{-1} using a KBr pellet technique.

Quantum chemistry methods

ChemDraw and Chem3D softwares attached to ChemOffice 2016 (Version: Ultra 16.0.0, PerkElmer informatics Inc., 2016) were used to optimize the molecular structure of PRX. The GAMESS package is a Hartree–Fock ab initio quantum chemistry package attached to Chem3D and was used to calculate molecular energy, charge distribution and bond order [20, 21]. The HF/6-31G level was used. The calculation accuracy and convergence threshold were the default values in all programs. All the calculations were completed using ordinary notebook computer.

Results and discussions

The thermal decomposition process of PRX

The thermal decomposition curves at nitrogen and air atmospheres obtained from the heating rate of 10 °C min^{-1} are shown in Fig. 1. It can be seen that the thermal decomposition of PRX in nitrogen and air atmospheres both undergo a two-stage process with the initial decomposition temperature of 198 °C (0.5% mass loss). In nitrogen, the first mass loss stage occurs from 198 to 293 °C, the DTG peak temperature is 249.9 °C, and the mass loss is 82.7%. Over 293 °C is the second stage, this is a very slow process of mass loss, and there is about 5.0% remnant at 800 °C. In air, the first mass loss stage is similar to in nitrogen atmosphere, occurs from 198 to 293 °C, the DTG peak temperature is 248.1 °C, and the mass loss is 85.2%. Over 293 °C is the second stage, and PRX decomposes completely at about 650 °C. Obviously, most of PRX decompose in the first stage, and the second stage is mainly pyrolysis of carbonaceous residue.

Before the decomposition of PRX, the DSC curves both show an obvious endothermic peak, and it implies that PRX melts before pyrolysis. In nitrogen, the DSC peak temperature is 194.9 °C, and the melting heat (peak area) is 87.8 J g^{-1}. In air, the DSC peak temperature is 194.5 °C, and the melting heat is 87.6 J g^{-1}. The DSC curves corresponding to the first mass loss step both show a small endothermic peak, and it suggests that the thermal pyrolysis process contains the intramolecular and intermolecular oxidation in nitrogen and air atmospheres. In nitrogen, there is no obvious heat effect on the DSC curve corresponding to the second stage, and it suggests that the

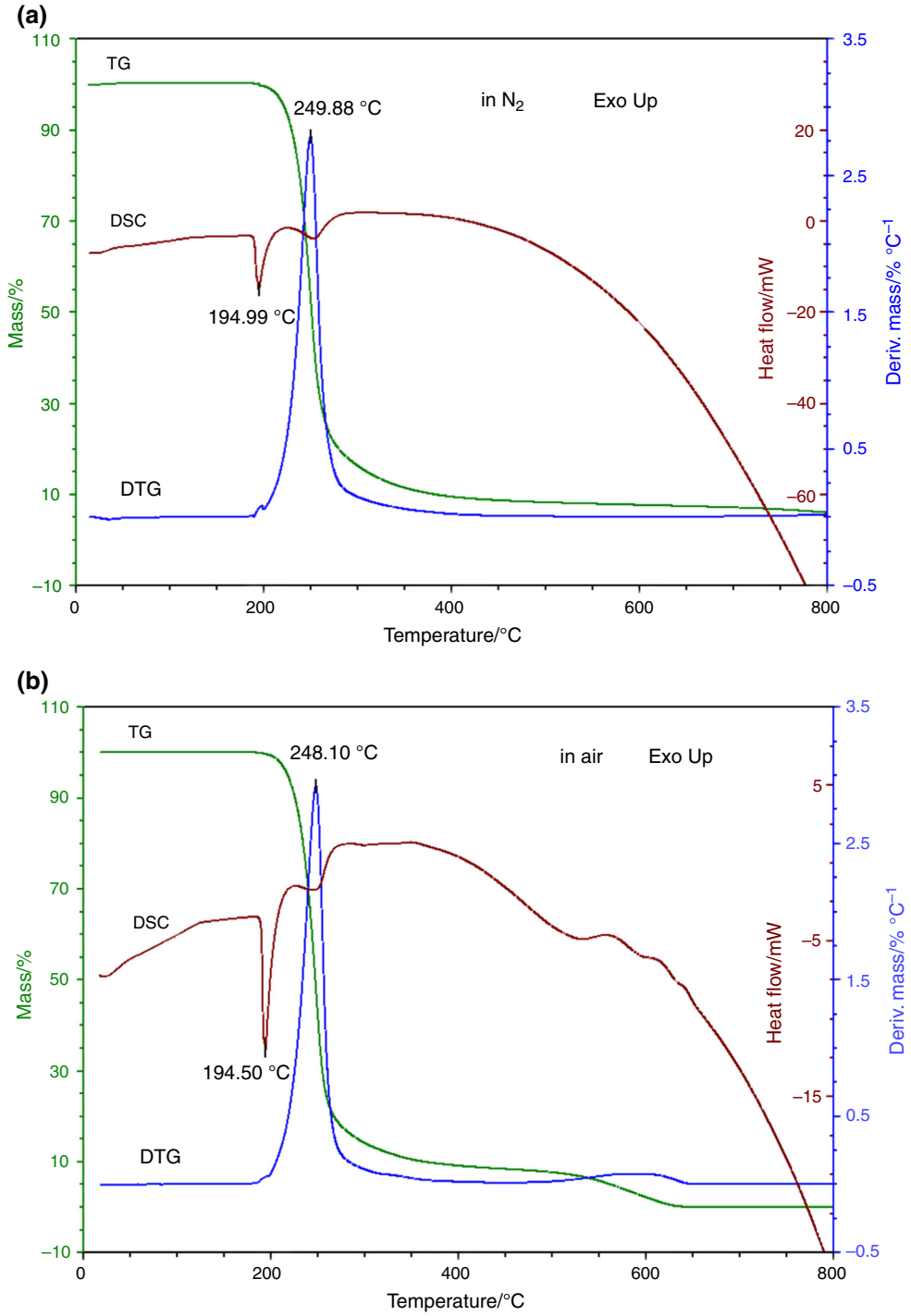

Fig. 1 The thermal analysis curves for PRX (heating rate: 10 °C min^{-1}). **a** In N_2 atmosphere, **b** in air atmosphere

second stage is a slow thermal pyrolysis process of carbonaceous residue. In air, the DSC curve corresponding to the later period of the second stage appears a smaller exothermic peak, and it indicates that the later period of the second stage is an oxidation (combustion) reaction process of carbonaceous residue. The thermal analytical curves in two atmospheres before 480 °C are almost exactly the same, and it means that the thermal decompositions of this period in two atmospheres are the same process. After 480 °C, the thermal decomposition in air is the fast oxidative decomposition (combustion) of carbonaceous residue.

The FTIR analysis of the gaseous species and the solid residues produced in the thermal degradation of PRX [22, 23]

The analysis of gaseous products generated by thermal decomposition provides valuable information on the mechanism of thermal decomposition. TG–FTIR is widely used to analyze the gaseous products generated by thermal decomposition [24, 25]. The three-dimensional diagrams of infrared absorption of evolved gas products obtained from PRX decomposition versus time and wavenumber during thermal decomposition are shown in Fig. 2. It can provide an overall perspective about evolved gas products during the thermal decomposition. From Fig. 2, it can be seen that in two atmospheres the gaseous products of the first half part (before 480 °C) of thermal decomposition are almost the same, although there is slight difference in the ratio of peak size, which means that the decomposition processes at this section in two atmospheres are the same. At the latter half part of decomposition processes, the gaseous products are very different in two atmospheres. The amount of the gaseous products is very small in nitrogenous atmosphere, and the amount of the gaseous products is very large in air atmosphere. The Gram–Schmidt (GS) curves of TG–FTIR

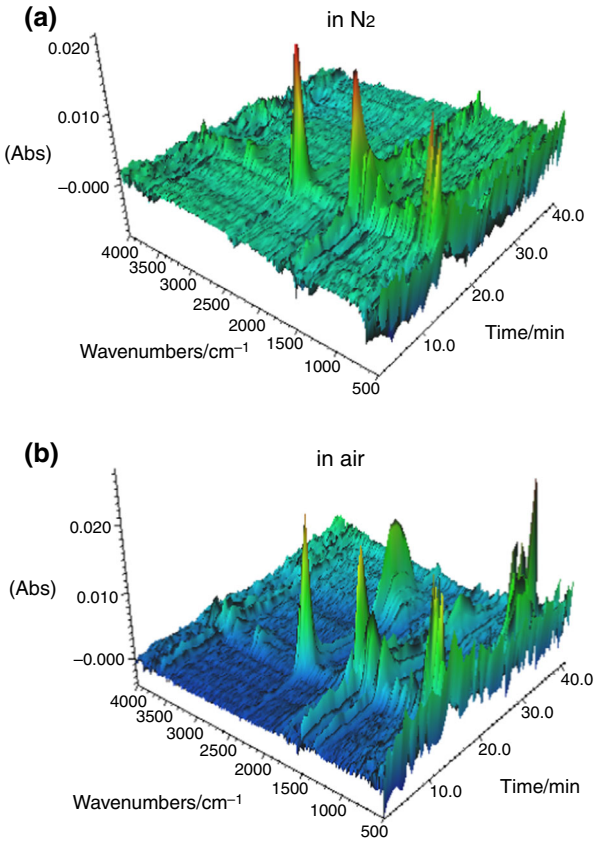

Fig. 2 3D TG–FTIR spectra of the evolved gaseous products of PRX. **a** In N_2 atmosphere, **b** in air atmosphere

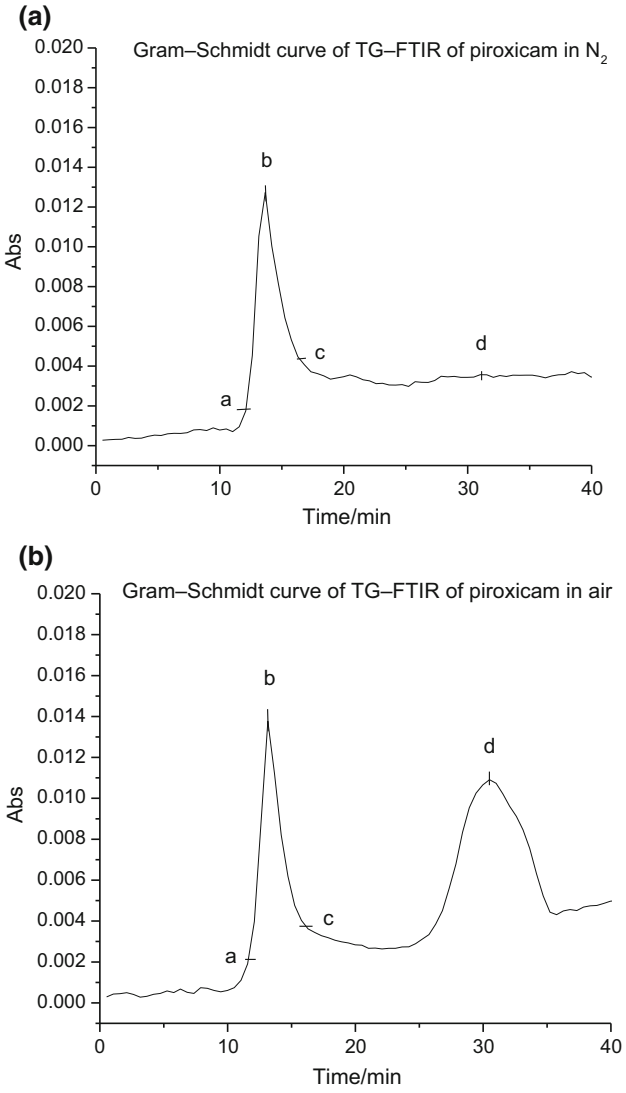

Fig. 3 Gram–Schmidt (GS) curves of the TG–FTIR of PRX. **a** In N_2 atmosphere, **b** in air atmosphere

are shown in Fig. 3. In contrast to Fig. 1, it can be seen that the GS curves both are similar to the DTG curves, and each GS peak corresponding to DTG peaks. The TG–FTIR spectra of the gaseous products obtained from different temperature during the thermal decomposition of PRX are shown in Fig. 4. From Fig. 4, it can be seen that the IR spectra of a, b, and c points (corresponding to the first DTG peak) in two atmospheres are similar with each other, just the peak sizes are different correspondingly. It means that the decomposition processes during the whole first stage are the same and successive, and the component of gaseous products are the same. It can be seen that the IR spectra of these points all contain H_2O bands (multiple bands near 3630 m^{-1}), unsaturation CH bands (3081 and 3030 cm^{-1}) of alkene, CO_2 bands (2356, 2284, and 669 cm^{-1}), C=N band (1613 cm^{-1}) of imine, C=C band (1442 cm^{-1}) of

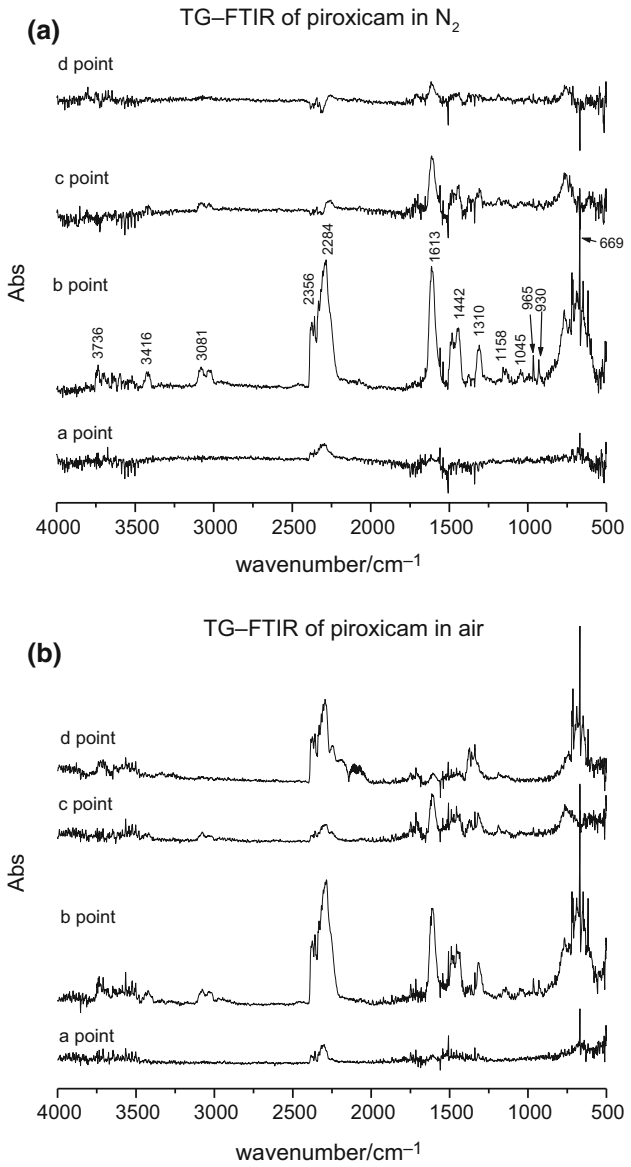

Fig. 4 The TG–FTIR spectra of the evolved gaseous products of PRX obtained at different temperatures (*a*, *b*, *c*, and *d* corresponding to Fig. 3). **a** In N_2 atmosphere, **b** in air atmosphere

alkene, SO_2 bands (broad peak 1310 and 1158 cm^{-1}) [26], and meanwhile the small NH_3 bonds (965 and 930 cm^{-1}) and C–O band (1045 cm^{-1}) can be seen. The big CO_2 bands and H_2O bands indicate that the pyrolysis process of PRX contains remarkable inter-molecule and intra-molecule oxidative reaction, and it is consistent with a small endothermic peak of DSC curves corresponding to the first mass loss step. The CO_2 bands, unsaturation CH bands, C=N band, C=C band, C–O band, and SO_2 band indicate that the all parts of PRX molecule, including sulfamide, amide, benzene ring and pyridine ring, all decompose simultaneously, namely the thermal decomposition of PRX is multiple site fracture process and most of PRX decompose directly to form gasifiable small molecules. The small NH_3 bonds indicate that part of tertiary amine is decomposed to form NH_3. The peaks of gaseous products at c point are very small, and it means that the larger proportion of the residue at this point is carbonaceous residue (char). The IR spectrum of d point in nitrogen indicates that the amount of gaseous products is very small at this time, and it means that the second stage of the thermal decomposition in nitrogen mainly is thermal cracking of carbonaceous residue. The IR spectrum of d point in air mainly contains H_2O, CO_2, CO (2112, and 2075 cm^{-1}) and SO_2 bands, and it means that the thermal decomposition of this moment in air is mainly oxidative decomposition reaction, and the main constituents of residues are mainly char and sulfide.

The infrared analysis of decomposition residues obtained from different temperatures can also provide direct information on the thermal degradation process. The IR spectra of PRX and residues obtained from different temperatures during thermal decomposition process in nitrogen atmosphere are shown in Fig. 5. It can be seen from Fig. 5 that the IR spectrum of residue obtained at the initial stage of thermal decomposition (205 °C) is roughly the same with that of PRX, but the bands of 1644, 1533, 1039, and 691 cm^{-1} are slightly reduced, and some bands shift slightly, for example, O–H band from 3393 moves to 3338 cm^{-1}, C=O band from 1644 moves to 1629 cm^{-1}, C=N and C=C bands from 1533 moves to 1530 cm^{-1}, and S=O band from 1355 moves to 1351 cm^{-1}. It means that the chemical environment of sulfamide, amide, and pyridine ring has changed. It can be seen from the IR spectrum of residue obtained at 245 °C (DTG peak of the first stage)

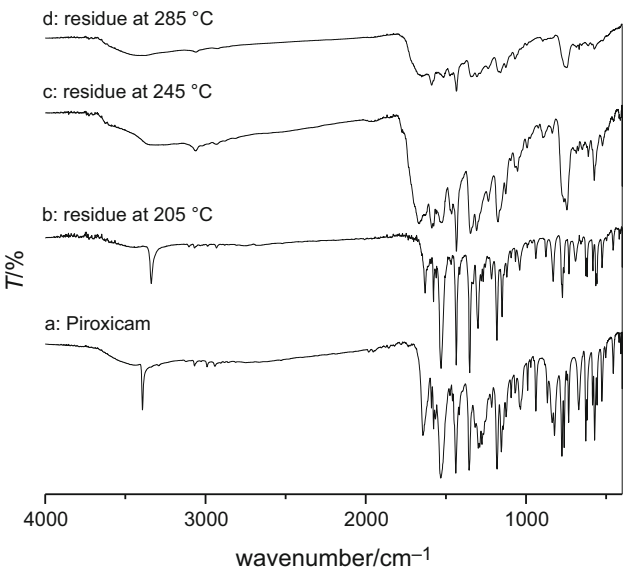

Fig. 5 IR Spectra of PRX and residues of PRX formed at the various temperatures

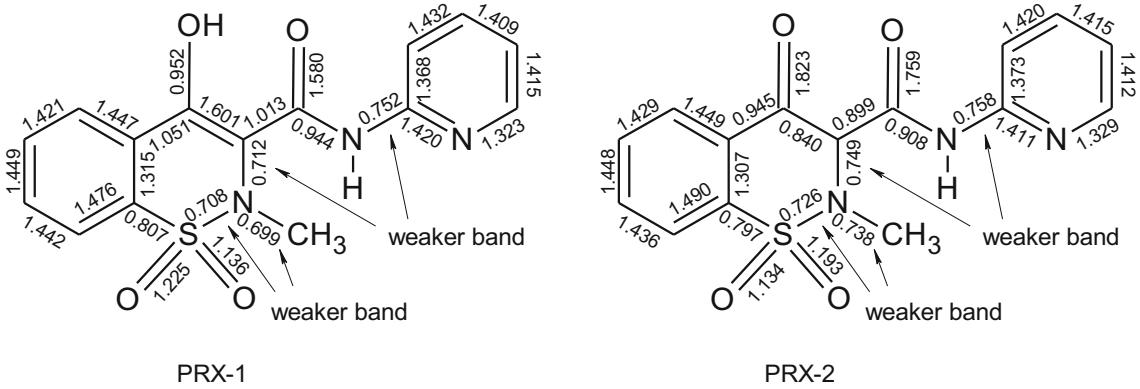

Scheme 1 Molecular bond orders of PRX

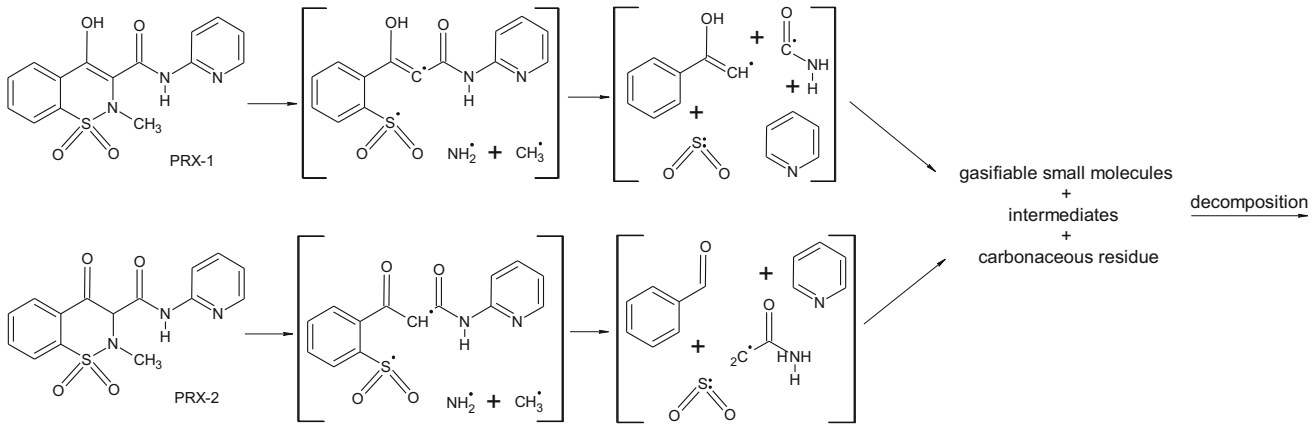

Scheme 2 The suggested thermal decomposition mechanism of PRX

that the O–H band disappear obviously, the C=O band, C=C band (1533 cm^{-1}) of benzene ring, C=N band (1533 cm^{-1}) of pyridine ring, and C–N band (1438 cm^{-1}) of the secondary amide group, S=O bands (1355 and 1154 cm^{-1}) of sulfamide, and C–OH band (1035 cm^{-1}) are decreased obviously. It proves again that sulfamide, amide, benzene ring, and pyridine ring decompose simultaneously at the first stage, and the PRX directly decompose to gasifiable small molecule. The visible bands at 1664, 1588, 1522, 1435, 1344, 1308, 1174, 1069, and 745 cm^{-1} indicate that there are heterocycle olefin, carbonyl, and sulfide in the residue. The IR spectrum of residue obtained at the second stage (285 °C) indicates that the organic compound structure all has been destroyed at this stage and, the residue mainly is char.

Thermal decomposition mode of PRX

Theoretically, the thermal decomposition of organic molecules is due to the molecular kinetic energy increasing during heating. These include atomic oscillations that rupture the weaker chemical bonds. Fracture occurs easier with lower orders of chemical bonds. Thermodynamically, the decomposition process also depends on the stability of the decomposition products or intermediates generated. In order to understand the thermal decomposition mode of PRX, a theoretical discussion is made from the perspective of the molecular structure. A quantum chemical ab initio method is used to calculate molecular charge distribution and the bond orders for PRX (Scheme 1). According to the molecular bond order distributions of PRX, the position and sequence of the chemical bonds ruptured could be judged, and the thermal decomposition mode of PRX in the thermal decomposition process could be speculated. As Refs. [27, 28] have been mentioned, PRX should have enol form (labeled as PRX-1) and keto form (labeled as PRX-2) structures. From Scheme 1, it can be seen that the weaker bonds of PRX-1 are the C–N bonds (0.699 and 0.712) and S–N bond (0.708) of sulfamide and C–N bond (0.752) of amide. The weaker bonds of PRX-2 are the S–N bond (0.726) and C–N bond (0.738 and 749) of sulfamide and C–N bond (0.758) of amide. The orders of these weaker bonds are so close, and they will rupture simultaneously in the initial stage of thermal decomposition. Then, the weaker

bonds of PRX-1, the C–S bonds (0.807) of sulfamide, the weaker bonds of PRX-2, the C–S bonds (0.797) of sulfamide, will also rupture and to make the sulfamide, amide and pyridine to decompose and to form small molecules and active radical intermediates. These small molecules will gasify at decomposition temperature and can be detected by TG–FTIR. Most of these active radical intermediates will further decompose into small molecules and be gasified, part of intermediates condensate into larger molecules or decompose into carbonaceous residue and remain in residue. Because of the oxidative activity of dioxide structure and sulfamide and the reaction active of radical intermediates, the inter-molecule and intra-molecule oxidative reaction occur simultaneously with thermal decomposition, and so, CO_2, SO_2, and H_2O can be detected by TG–FTIR during the thermal decomposition. There are part of benzene and pyridine remaining in residue in the early stages of thermal decomposition due to their more stable structure.

Based on the above comprehensive analyses and quantum chemical calculation, speculated thermal decomposition mechanism of PRX is shown in Scheme 2.

Conclusions

The thermal decomposition mechanism of PRX was studied by thermal analytical technology, FTIR spectroscopy and quantum chemistry method. The results indicated that the thermal decomposition of PRX is a two-stage process with the initial temperature of 198 °C in either nitrogen or air atmospheres. The first stages of thermal decompositions in two atmospheres are the same process. The main part of the molecule, including sulfamide, amide, benzene ring and pyridine ring, decompose simultaneously and to form gasifiable small molecules and carbonaceous residue in the first stage. The second stage in nitrogen is a slow thermal pyrolysis process of carbonaceous residue. The forepart of the second stage in air is a slow thermal pyrolysis process as like as in nitrogen, and the later period of the second stage is an oxidation (combustion) reaction process of carbonaceous residue. PRX is stable under ambient temperature and air atmosphere, and it can be preserved for long-term storage under ambient temperature and air atmosphere.

References

1. March L, Smith EU, Hoy DG, Cross MJ, Sanchez-Riera L, Blyth F, Buchbinder R, Vos T, Woolf AD. Burden of disability due to musculoskeletal (MSK) disorders. Best Pract Res Clin Rheumatol. 2014;28:353–66.
2. Glyn-Jones S, Palmer AJ, Agricola R, Price AJ, Vincent TL, Weinans H, Carr AJ. Osteoarthritis. Lancet. 2015;386:376–87.
3. Buckland-Wright C. Subchondral bone changes in hand and knee osteoarthritis detected by radiography. Osteoarthr Cartil. 2004;18:S10–9.
4. Pelletier JP. Efficacy and safety of oral NSAIDs and analgesics in the management of osteoarthritis: evidence from real-life setting trials and surveys. Semin Arthritis Rheum. 2016;45:S22–7.
5. Richardson CJ, Blocka KL, Ross SG, Verbeeck RK. Effects of age and sex on piroxicam disposition. Clin Pharmacol Ther. 1985;37:13–8.
6. Eichstadt LR, Moore GE, Childress MO. Risk factors for treatment-related adverse events in cancer-bearing dogs receiving piroxicam. Vet Comp Oncol. 2017;15(4):1346–53.
7. Kovala-Demertzi D. Recent advances on non-steroidal anti-inflammatory drugs, NSAIDs: organotin complexes of NSAIDs. J Organomet Chem. 2006;691:1767–74.
8. Tita B, Stefanescu M, Tita D. Complex of anti-inflammatory non-steroidal drugs from oxicam family. 1. Synthesis and characterization of Zn (II) complex with Piroxicam. Rev Chim (Bucuresti). 2011;62(10):1002–7.
9. Dutta S, Padhye S, Mckee V. Structural characterization and SOD activity of copper–oxaprozinate. Inorg Chem Commun. 2004;7:1071–4.
10. Ledeti A, Olariu T, Caunii A, Vlase G, Circioban D, Baul B, Ledeti I, Vlase T, Murariu M. Evaluation of thermal stability and kinetic of degradation for levodopa in non-isothermal conditions. J Therm Anal Calorim. 2018;131(2):1881–8.
11. Cartaxo-Furtado NAD, de Castilho ARF, Freires IA, Santana CP, Sampaio TO, Xavier MA, de Medeiros ACD, Alves HD, Costa EMMD, Rosalen PL, Pereira JV. Physicochemical characterization of a new raw material obtained from leaves of *Syzygium cumini* (L.) Skeel (Myrtaceae). J Therm Anal Calorim. 2017;127(2):1137–41.
12. Tak SR, Sohn YT. Crystal forms of a new 5-HT4 receptor agonist DA-6886. J Therm Anal Calorim. 2016;123(3):2477–83.
13. Correa JCR, Perissinato AG, Serra CHD, Trevisan MG, Salgado HRN. Polymorphic stability of darunavir and its formulation. J Therm Anal Calorim. 2016;123(3):2185–90.
14. Ledeti I, Bolintineanu S, Vlase G, Circioban D, Ledeti A, Vlase T, Suta LM, Caunii A, Murariu M. Compatibility study between antiparkinsonian drug Levodopa and excipients by FTIR spectroscopy, X-ray diffraction and thermal analysis. J Therm Anal Calorim. 2017;130(1):433–41.
15. Attia AK, Mohamed GG, Ahmed HE. Structural investigation, molecular structure and molecular docking of solifenacin succinate, flavoxate hydrochloride and tolterodine tartrate anticholinergic drugs. J Therm Anal Calorim. 2018;131(2):1345–60.
16. Jimenez JJ, Munoz BE, Sanchez MI, Pardo R. Forced and long-term degradation assays of tenoxicam, piroxicam and meloxicam in river water. Degradation products and adsorption to sediment. Chemosphere. 2018;191:903–10.
17. Aminuddin M, Nazim U, Ahmad I. Photo- and thermal degradation of piroxicam in aqueous solution. Indian J Pharm Sci. 2012;73(4):387–91.
18. Modhave DT, Handa T, Shah RP, Singh S. Successful characterization of degradation products of drugs using LC–MS tools: application to piroxicam and meloxicam. Anal Methods. 2011;3(12):2864–72.
19. Tiţa B, Marian E, Fuliaş A, Jurca T, Tiţa D. Thermal stability of piroxicam. J Therm Anal Calorim. 2013;112(1):367–74.
20. Schmidt MW, Baldridge KK, Boatz JA, Elbert ST, Gordon MS, Jensen JJ, Koseki S, Matsunaga N, Nguyen KA, Su S, Windus TL, Dupuis M, Montgomery JA. General atomic and molecular electronic structure system. J Comput Chem. 1993;14:1347–63.

21. Alexeev Y, Mazanetz MP, Ichihara O, Fedorov DG. GAMESS as a free quantum-mechanical platform for drug research. Curr Top Med Chem. 2012;12(18):2013–33.
22. Xie JX, Chang JB, Wang XM. Applications of infrared spectroscopy in organic chemistry and medicinal chemistry. Beijing: Science Press; 2001 **(in Chinese)**.
23. NIST Chemistry Web book Standard Reference Database, 2011, 69 release. http://webbook.nist.gov/chemistry.
24. Wu CJ, You JZ, Wang XJ. Study on the thermal decomposition of famciclovir. J Therm Anal Calorim. 2018;131(2):1361–71.
25. Gallo RC, Ferreira APG, Castro REA, Cavalheiro ETG. Studying the thermal decomposition of carvedilol by coupled TG–FTIR. J Therm Anal Calorim. 2016;123(3):2307–12.
26. Mohamed GG, El-Sherif AA, Saad MA, El-Sawy SEA, Morgan SM. Mixed-ligand complex formation of tenoxicam drug with some transition metal ions in presence of valine: synthesis, characterization, molecular docking, potentiometric and evaluation of the humeral immune response of calves. J Mol Liq. 2016;223:1311–32.
27. Raja MU, Tauchman J, Therrien B, Süss-Fink G, Riedel T, Dyson PJ. Arene ruthenium and pentamethylcyclopentadienyl rhodium and iridium complexes containing *N*, *O*-chelating ligands derived from piroxicam: synthesis, molecular structure and cytotoxicity. Inorg Chim Acta. 2014;409:479–83.
28. de Souza KF, Martins JA, Pessine FB, Custodio R. A theoretical and spectroscopic study of conformational structures of piroxicam. Spectrochim Acta A. 2010;75(2):901–7.